JBC RESEARCH ARTICLE

Nitration of protein kinase G-Iα modulates cyclic nucleotide crosstalk *via* phosphodiesterase 3A: Implications for acute lung injury

Received for publication, December 7, 2020, and in revised form, June 22, 2021 Published, Papers in Press, July 10, 2021,
https://doi.org/10.1016/j.jbc.2021.100946

Evgeny A. Zemskov[1,‡], Xiaomin Wu[1,‡], Saurabh Aggarwal[2,‡], Mannivannan Yegambaram[1], Christine Gross[2], Qing Lu[1], Hui Wang[1,3], Haiyang Tang[1,3,4], Ting Wang[4,5,6], and Stephen M. Black[4,6,7,*]

From the [1]Department of Medicine, The University of Arizona Health Sciences, Tucson, Arizona, USA; [2]Vascular Biology Center, Augusta University, Augusta, Georgia, USA; [3]College of Veterinary Medicine, Northwest A&F University, Yangling, Shaanxi, China; [4]Center for Translational Science, Florida International University, Port Saint Lucie, Florida, USA; [5]Department of Internal Medicine, The University of Arizona, Phoenix, Arizona, USA; [6]Department of Environmental Health Sciences, Robert Stempel College of Public Health and Social Work, [7]Cellular Biology & Pharmacology, Herbert Wertheim College of Medicine, Florida International University, Miami, Florida, USA

Edited by Dennis Voelker

Phosphodiesterase 3A (PDE3A) selectively cleaves the phosphodiester bond of cAMP and is inhibited by cGMP, making it an important regulator of cAMP–cGMP signaling crosstalk in the pulmonary vasculature. In addition, the nitric oxide–cGMP axis is known to play an important role in maintaining endothelial barrier function. However, the potential role of protein kinase G-Iα (PKG-Iα) in this protective process is unresolved and was the focus of our study. We describe here a novel mechanism regulating PDE3A activity, which involves a PKG-Iα–dependent inhibitory phosphorylation of PDE3A at serine 654. We also show that this phosphorylation is critical for maintaining intracellular cAMP levels in the pulmonary endothelium and endothelial barrier integrity. In an animal model of acute lung injury (ALI) induced by challenging mice with lipopolysaccharide (LPS), an increase in PDE3 activity and a decrease in cAMP levels in lung tissue was associated with reduced PKG activity upon PKG-Iα nitration at tyrosine 247. The peroxynitrite scavenger manganese (III) tetrakis(1-methyl-4-pyridyl)porphyrin prevented this increase in PDE3 activity in LPS-exposed lungs. In addition, site-directed mutagenesis of PDE3A to replace serine 654 with alanine yielded a mutant protein that was insensitive to PKG-dependent regulation. Taken together, our data demonstrate a novel functional link between nitrosative stress induced by LPS during ALI and the downregulation of barrier-protective intracellular cAMP levels. Our data also provide new evidence that PKG-Iα is critical for endothelial barrier maintenance and that preservation of its catalytic activity may be efficacious in ALI therapy.

Second messengers, cAMP and cGMP, play key roles in many aspects of cell signaling (1). In the pulmonary vasculature, cAMP and cGMP are involved in regulating cytoskeletal structural remodeling in both endothelial and smooth muscle cells and as such can regulate endothelial barrier permeability and vasorelaxation (2–6). Downstream, the cyclic nucleotide effectors, cAMP-dependent PKA and cGMP-dependent protein kinase G-1α (PKG-Iα) can directly regulate the endothelial barrier function *via* the phosphorylation of proteins responsible for the cytoskeleton remodeling (2, 5, 7, 8). Acute lung injury (ALI) and acute respiratory distress syndrome (ARDS) are characterized by acute development of respiratory failure, bilateral diffuse lung infiltrations, and hypoxemia because of endothelial barrier dysfunction and hyperpermeability (reviewed in Ref. (9)). Endothelial hyperpermeability is associated with endothelial cytoskeleton rearrangement: disassembly of cortical actin and actin stress fiber formation, which serve as contractile force (6, 10). Numerous publications have demonstrated protective effects of cAMP–cGMP-stimulating compounds or inhibitors of cyclic nucleotide–specific phosphodiesterases (PDEs) in cellular and animal models of ALI–ARDS as well as chronic pulmonary diseases (11–15). Excessive generation of reactive oxygen species and reactive nitrogen species leading to oxidative and nitrosative stress is characteristic for ALI–ARDS pathology (reviewed in Ref. (9)). Peroxynitrite, produced by uncoupled endothelial nitric oxide synthase, can induce protein tyrosine nitration altering individual protein function. We have recently shown that a key regulator of the barrier-disrupting actin skeleton remodeling, small GTPase RhoA, is nitrated in LPS-challenged cells. This tyrosine nitration activates RhoA and exacerbates the barrier-disruptive effect of LPS (16). In contrast, PKG-Iα can be modified by tyrosine nitration at tyrosine 247 (Y^{247}), and this nitration event inhibits its enzymatic activity (17). Furthermore, in a series of studies, we have confirmed the important role played by nitrosative

‡ These authors contributed equally to this work.
* For correspondence: Stephen M. Black, stblack@fiu.edu.
Present address for Saurabh Aggarwal: Department of Anesthesiology, The University of Alabama, Birmingham, Alabama, USA.
Present address for Christine Gross: Department of Medicine at Broward Health Medical Center, Fort Lauderdale, Florida, USA.

stress in the development of ALI (17–19). Thus, the goal of this study was to determine if the nitration-mediated inhibition of PKG-Iα is involved in the barrier disruption associated with ALI.

Cyclic nucleotide–specific PDEs efficiently downregulate cAMP-activated or cGMP-activated signaling pathways by degrading their respective cyclic nucleotides. There is significant diversity in PDE superfamily members that include differences in their substrate specificity and kinetics, tissue distribution, intracellular localization, enzymatic activity regulation, and others (20–22). This along with the presence of multiple PDE isoforms creates a complex multilevel signaling network (21, 23). Phosphodiesterase 3 (PDE3), a cGMP–cAMP-specific PDE, is ubiquitously expressed in mammalian tissues (24). Two isoforms of PDE3 encoded by *PDE3A* and *PDE3B* genes differ in their tissue specificity. PDE3A is expressed in heart and lungs, whereas PDE3B is detected in other organs such as the liver and fat pad (24). Increased PDE3 activity has also been correlated with lung pathological conditions such as chronic obstructive pulmonary disease (25). As a PDE with dual specificity, PDE3 is intimately involved in cyclic nucleotide crosstalk (26, 27). In this study, we demonstrate a new aspect of PDE3A regulation related to cAMP–cGMP crosstalk that is mediated by a PKG-Iα–dependent inhibitory phosphorylation at serine 654 (S^{654}). Furthermore, our study links this PDE3A–PKG-Iα functional axis to the development of ALI. We show that the peroxynitrite generated in the lungs of LPS-challenged mice negatively regulates cAMP levels *via* the activation of PDE3A. This activation is the result of the nitration-mediated inhibition of PKG-Iα and a subsequent decrease in PKG-dependent PDE3A phosphorylation.

Results

Three families of PDEs can regulate cAMP–cGMP crosstalk in the vasculature: phosphodiesterase 2 (PDE2), PDE3, and phosphodiesterase 5 (PDE5) (26–28). Thus, our initial experiments aimed to evaluate protein levels and enzymatic activities of these PDEs in mouse lung exposed to LPS. Our data indicate that LPS exposure does not alter the protein levels of PDE2, PDE3A, or PDE5 (Fig. 1, *A–C*, respectively) in the mouse lung. However, certain PDE enzymatic activities were modulated by LPS. Although PDE2 activity was not altered (Fig. 1*D*), the activity of PDE3 was significantly increased (Fig. 1*E*), whereas PDE5 was significantly reduced (Fig. 1*F*). Furthermore, we identified dramatic changes in the levels of the second messenger levels cAMP and cGMP such that cAMP levels were significantly attenuated (Fig. 1*G*), whereas the levels of cGMP were significantly increased (Fig. 1*H*). It is

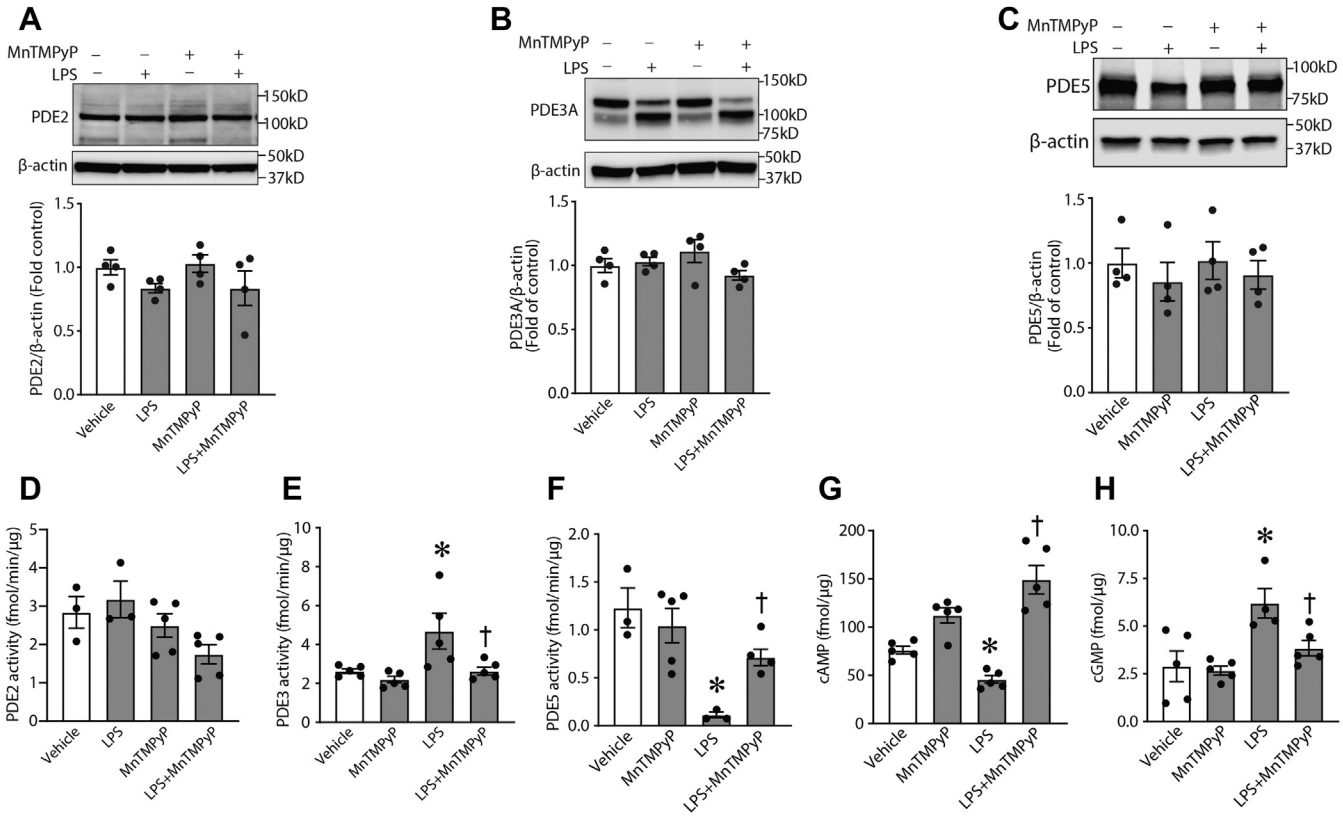

Figure 1. Altered phosphodiesterase (PDE) activities and cyclic nucleotide levels in LPS-induced animal model of ALI. Lungs were isolated from mice treated with LPS and/or MnTMPyP as described in the Experimental procedures section. The tissue extracts were used to evaluate the protein levels of PDE2, PDE3, and PDE5 (*A–C*) and respective activities (*D–F*). LPS increases PDE3 activity and a decrease in PDE5 activity, despite no changes in protein levels. PDE activity changes were sensitive to MnTMPyP pretreatment indicative of a peroxynitrite-dependent mechanism. LPS decreased cAMP levels (*G*), whereas cGMP levels were increased (*H*). MnTMPyP pretreatment prevented these changes (*G* and *H*). Data represent mean ± SEM, n = 3 to 5. *$p < 0.05$ *versus* control lungs; †$p < 0.05$ *versus* LPS alone. ALI, acute lung injury; LPS, lipopolysaccharide; MnTMPyP, manganese (III) tetrakis(1-methyl-4-pyridyl)porphyrin.

likely that the elevation of cGMP levels is linked to the inhibition of cGMP-specific PDE5 we observed (Fig. 1*F*), whereas an activation of cAMP-specific PDE3 leads to cAMP level decrease (Fig. 1*E*). Since PDE3A is the only PDE3 isoform expressed in lung tissue (24), we assume that PDE3 activity in our experiments can be attributed to this isoform. Nitrosative stress is characteristic for *in vitro* and *in vivo* models of ALI (16–19, 29, 30) where it is associated with alterations in protein–enzyme functions because of protein tyrosine nitration (16, 17). To explore a possible link between reactive nitrogen species generation and changes in cAMP–cGMP levels and PDE activities in lungs of LPS-challenged mice, we pretreated a group of animals with a peroxynitrite scavenger, manganese (III) tetrakis(1-methyl-4-pyridyl)porphyrin (MnTMPyP). Data obtained clearly demonstrated that changes in cAMP and cGMP levels detected in LPS-challenged mice were peroxynitrite dependent: MnTMPyP pretreatment significantly diminished this effect of LPS (Fig. 1, *G* and *H*). Moreover, MnTMPyP efficiently reversed the levels of PDE activities induced by LPS (Fig. 1, *D*–*F*), suggesting that peroxynitrite-dependent modifications of cyclic nucleotide signaling exist in ALI.

LPS-induced nitrosative stress modulates cyclic nucleotide–dependent protein kinase activity in the mouse lung

Significant changes in PDE activities and cyclic nucleotide levels in the lungs of LPS-challenged mice may affect functions of the downstream effectors, cAMP-dependent and cGMP-dependent protein kinases (PKA and PKG-Iα). This, in turn, may have critical consequences for vascular permeability *in vivo*. To study these possible effects of LPS, we evaluated protein levels and enzymatic activities of the respective protein kinases. Our data demonstrate that, while the protein levels of PKG-Iα (Fig. 2*A*) and PKA (Fig. 2*D*) were unchanged by LPS treatment, their activities were impaired in LPS-treated lungs. Both PKG activity (Fig. 2, *B* and *C*) and PKA activity (Fig. 2*E*) were significantly decreased. Importantly, treatment of LPS-challenged mice with MnTMPyP attenuated the LPS-induced decrease in PKG and PKA activity (Fig. 2, *B*, *C*, and *E*) without any significant effect on their protein levels (Fig. 2, *A* and *D*). Together, these results indicate that nitrative stress plays an important role in the modulation of enzymatic activities of cAMP-dependent and cGMP-dependent protein kinases in ALI.

PKG-Iα nitration is increased in lung tissue of LPS-challenged mice

LPS-induced signaling increased peroxynitrite levels *in vivo*, as determined by the oxidation of dihydrorhodamine 123 (DHR123) to rhodamine 123, whereas MnTMPyP abrogated an accumulation of peroxynitrite in LPS-exposed tissue (Fig. 3*A*). Using 3-nitrotyrosine–specific antibody, we were able to detect a significant increase in PKG-Iα nitration (Fig. 3*B*). We have previously reported that PKG-Iα is susceptible to nitration at Y^{247} and that this modification impairs PKG activity (17), and using an antibody developed specifically against nitrated Y^{247} of PKG-Iα (17), we also found a significant increase in this PKG-Iα modification in PKG-Iα–transfected human embryonic kidney 293T (HEK293T) cells exposed to the peroxynitrite generator, 3-morpholinosydnonimine (Fig. 3*C*) and, more importantly, in mouse lungs exposed to LPS (Fig. 3*D*). Specificity was again validated by our data showing that DHR123 oxidation and PKG-Iα nitration were attenuated by MnTMPyP (Fig. 3).

Identification of a novel PKG-specific phosphorylation site in PDE3A involved in regulating PDE3A activity

To study possible effects of PKG-Iα on PDE3A function, we first determined if a physical association exists between the two proteins. To accomplish this, we overexpressed PKG-Iα in HEK293T cells, and using immunoprecipitation (IP) analysis, we were able to demonstrate an association of PKG-Iα and PDE3A in a pulled-down protein complex, which may suggest

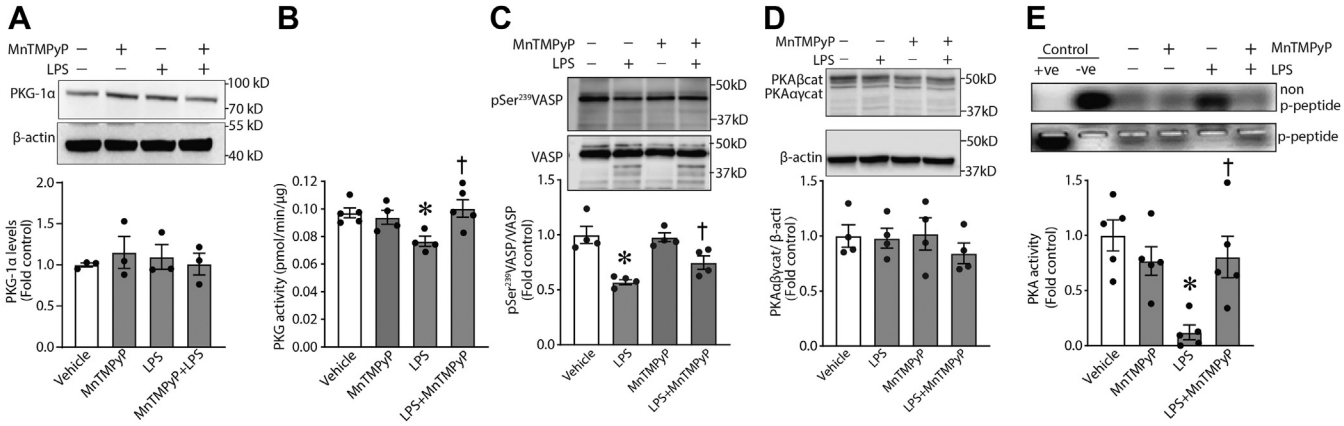

Figure 2. LPS treatment impairs PKA and PKG activities *in vivo via* peroxynitrite-dependent mechanism. The activity of PKA and PKG was tested in lung extracts obtained from mice treated with LPS and/or MnTMPyP as described in the Experimental procedures section. The protein levels of respective enzymes were evaluated by immunoblotting. LPS treatment did not affect the protein levels of either PKG-Iα (*A*) or PKA (*D*). However, LPS attenuated both PKG-Iα (*B* and *C*) and PKA (*E*) activity. Again, MnTMPyP pretreatment preserved the activity of PKA and PKG (*B*, *C*, and *E*). Data are mean ± SEM, n = 3 to 5. *$p < 0.05$ *versus* control lungs; †$p < 0.05$ *versus* LPS alone. LPS, lipopolysaccharide; MnTMPyP, manganese (III) tetrakis(1-methyl-4-pyridyl)porphyrin; PKG, protein kinase G.

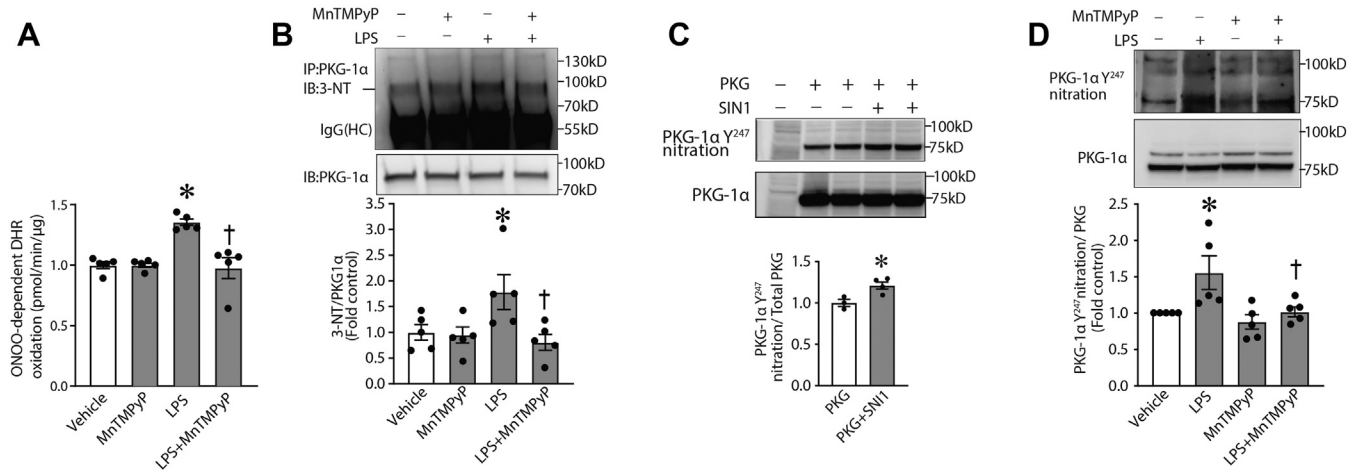

Figure 3. Nitrosative stress induced by LPS *in vivo* leads to PKG-Iα tyrosine nitration. *A*, peroxynitrite levels, estimated using DHR oxidation, were significantly increased in LPS-treated mice. Specificity of signal was demonstrated by MnTMPyP pretreatment attenuating DHR123 oxidation. *B*, immunoprecipitation analysis using an antibody specific to nitrotyrosine (3-NT) demonstrated an increase in the tyrosine nitration of PKG-Iα immunoprecipitated from LPS-exposed tissues. MnTMPyP pretreatment prevented the nitration of PKG-Iα. IgG (HC) is the immunoglobulin heavy chain. *C*, immunoblotting using an antibody specific to nitro-Y^{247} in PKG-Iα confirmed the increase in PKG-Iα nitration in HEK293T cells transfected with a PKG-Iα expression plasmid and treated with 3-morpholinosydnonimine. *D*, an increase in PKG-Iα nitration in mouse lungs exposed to LPS was also shown to occur at Y^{247}. MnTMPyP reduced Y^{247} nitration in PKG-Iα in response to LPS. Data represent mean ± SEM, n = 3 to 5. *$p < 0.05$ *versus* control lungs; †$p < 0.05$ *versus* LPS alone. DHR, dihydrorhodamine; HEK293T, human embryonic kidney 293T cells; LPS, lipopolysaccharide; MnTMPyP, manganese (III) tetrakis(1-methyl-4-pyridyl)porphyrin; PKG-Iα, protein kinase G-Iα; Y^{247}, tyrosine 247.

an interaction between the enzymes (Fig. 4*A*). Furthermore, this association between PDE3A and PKG-Iα correlated with a decrease in PDE3 activity (Fig. 4*B*) and an increase in cAMP levels (Fig. 4*C*). Taken together, these data suggest that PDE3A may be phosphorylated by PKG-Iα, and this phosphorylation regulates PDE3A activity toward cAMP. To further investigate this possibility, we performed database searches in order to reveal putative PKG-dependent phosphorylation sites in the PDE3A primary structure using NetPhos 3.1 (DTU Bioinformatics). Several PKG-specific phosphorylation sites conserved in human and mouse PDE3A amino acid sequences were predicted (Fig. 4*D*). To validate these PKG-Iα–specific post-translational modifications, we then used MS analysis. To accomplish this, HEK293T cells were transfected with expression plasmids containing PDE3A and PKG-Iα complementary DNAs (Fig. 5*A*). PDE3A was then immunopurified from the cell lysates, separated by SDS-PAGE and in-gel trypsinized. MS analysis was performed on the extracted peptides. Our results identified S^{654} phosphorylation in PDE3A in cells overexpressing PKG-Iα (Fig. 5, *B* and *C*). To further validate this PKG-dependent PDE3A phosphorylation site, we generated an antibody to specifically recognize p-S^{654} in PDE3A. Using this antibody, we were able to demonstrate an increase in p-$S^{654\text{-PDE3A}}$ when PDE3A was coexpressed with PKG-Iα in HEK293T cells (Fig. 5*D*). Using this antibody, we were also able to detect an abundant phosphorylation of PDE3A at S^{654} in the mouse lung and importantly demonstrate that LPS challenge dramatically decreases this post-translational modification (Fig. 5*E*). To study the possible regulatory role of PKG-Iα–mediated phosphorylation of PDE3A at S^{654}, we generated a PDE3A mutant in which S^{654} was replaced by alanine (S^{654}A-PDE3A) and tested its

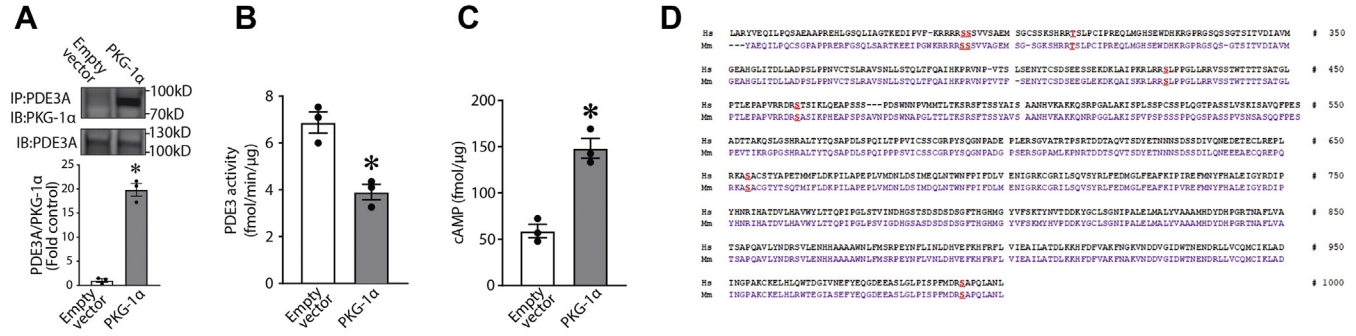

Figure 4. Expression of PKG-Iα downregulates PDE3A activity and increases cAMP levels *in vitro*. PKG-Iα was transiently expressed in PKG-Iα–deficient HEK293T cells; as a negative control, the cells were transfected with an empty vector. *A*, immunoprecipitation analysis identified an association of PDE3A with PKG-Iα. PKG-Iα–expressing cells also exhibit a significant decrease in PDE3 activity (*B*) and a significant increase in cAMP levels (*C*). Data represent mean ± SEM, n = 3. *$p < 0.05$ *versus* empty vector. *D*, comparative analysis of human and mouse PDE3A amino acid sequences using NetPhos 3.1 revealed conserved PKG-specific phosphorylation sites (shown in *red*). HEK293T, human embryonic kidney 293T cells; PDE3A, phosphodiesterase 3A; PKG-Iα, protein kinase G-Iα.

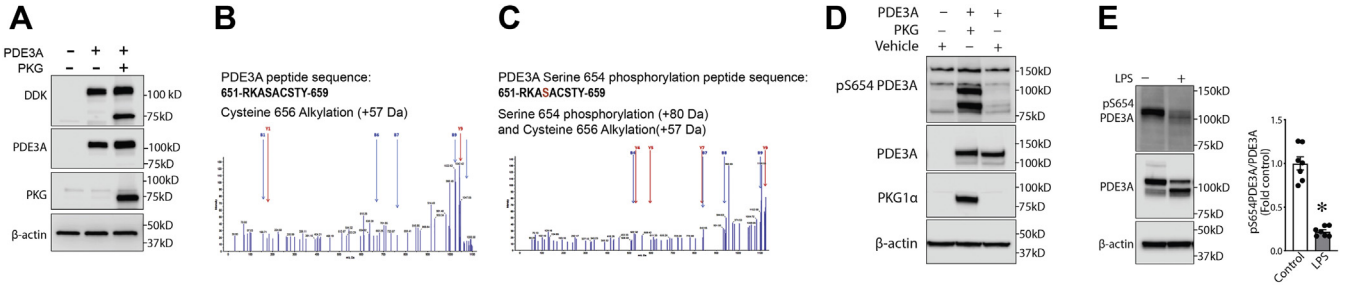

Figure 5. PKG-Iα phosphorylates PDE3A at S^{654}. HEK293T cells were transfected with an expression plasmid for PDE3A either alone or cotransfected with a PKG-Iα expression plasmid. Then cell lysates were subjected to PDE3A immunoprecipitation followed by SDS-PAGE and MALDI-TOF MS analysis as described in the Experimental procedures section. *A*, transfection and expression of PDE3A and PKG-Iα in HEK293T cells were confirmed by immunoblotting using antibodies against FLAG-tag, PDE3A, and PKG-Iα. *B* and *C*, MS/MS identified a PDE3A-specific peptide containing a serine located at position 654 (predicted PKG phosphorylation site) that was only phosphorylated when cells were transfected with PDE3A and PKG-Iα. *D*, the antibody generated against PKG-specific phosphorylation site, phospho-S^{654} in PDE3A, specifically recognized this modification when PDE3A expressed with PKG-Iα in HEK293T cells and did not react with PDE3A expressed alone. *E*, the antibody specific to phospho-S^{654}-PDE3A demonstrated dramatic changes of this PDE3A modification in mouse model of ALI. Data represent mean ± SEM, n = 7. *$p < 0.05$ control *versus* lipopolysaccharide (LPS)-treated mice. HEK293T, human embryonic kidney 293T cells; PDE3A, phosphodiesterase 3A; PKG-Iα, protein kinase G-Iα; S^{654}, serine 654.

functional regulation *in vitro*. myc-DDK-tagged wtPDE3A or the S^{654}A-PDE3A mutant was expressed in the presence or the absence of PKG-Iα in HEK293T cells. IP analysis showed that both wtPDE3A and the S^{654}A-PDE3A mutant efficiently interacted with PKG-Iα (Fig. 6*A*). wtPDE3A was also phosphorylated at S^{654}, when the cells expressing wtPDE3A were simultaneously transfected with PKG-Iα (Fig. 6*B*). However, the S^{654}A-PDE3A–PKG-Iα interaction (Fig. 6*A*) did not lead to S^{654}A-PDE3A mutant phosphorylation (Fig. 6*B*). The phosphorylation of wtPDE3A by PKG-Iα correlated with a decrease in wtPDE3 activity (Fig. 6*C*) and a subsequent increase in cAMP levels (Fig. 6*D*). In contrast, the activity of the phospho-null S^{654}A-PDE3A mutant (Fig. 6*C*) was unaffected, and cAMP levels (Fig. 6*D*) were unchanged in the presence of PKG-Iα. Together, these data clearly indicate that S^{654} is a previously unidentified PKG-dependent phosphorylation site in PDE3A that negatively regulates PDE3A activity.

Discussion

Stimulation of soluble guanylate cyclases by nitric oxide or nitric oxide–independent activators leads to intracellular cGMP elevation and PKG-Iα activation. Moreover, soluble guanylate cyclase activation is accompanied by an increase in cAMP levels and PKA activity (31–33). This suggests direct crosstalk between cGMP-dependent and cAMP-dependent pathways. However, the molecular mechanisms underlying this crosstalk are not completely understood. PKG-Iα is a well-known cGMP-dependent modulator of vasorelaxation, which acts, in part, *via* phosphorylation of actin cytoskeleton–

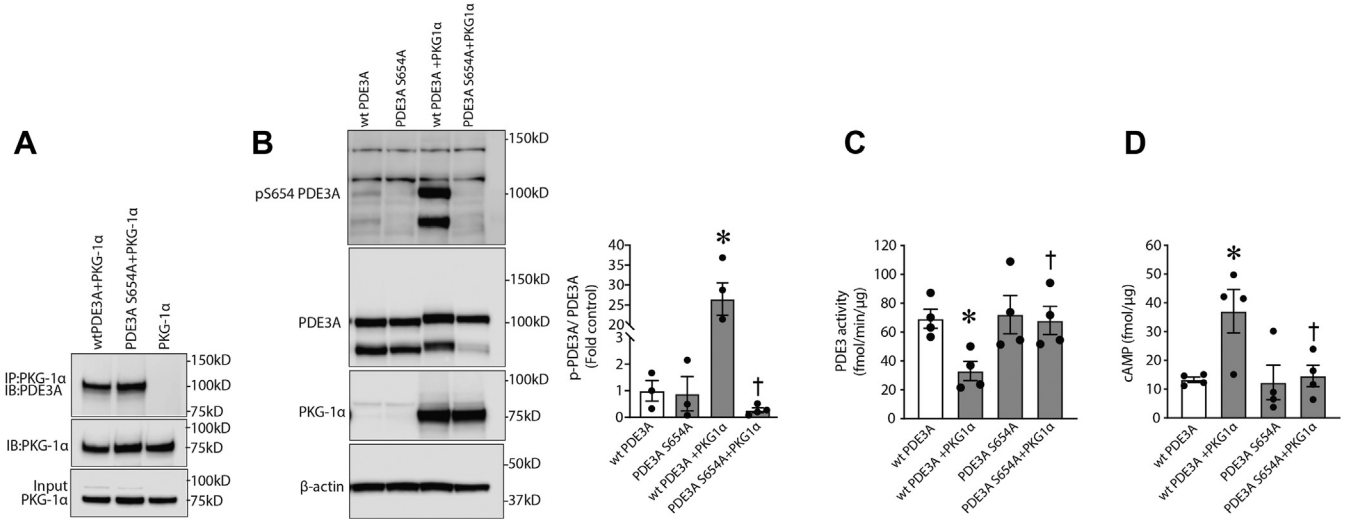

Figure 6. PKG-Iα–dependent phosphorylation of PDE3A at S^{654} inhibits PDE3A activity and protects intracellular cAMP from degradation. *A*, in HEK293T cells, overexpressed PKG-Iα associates with both wtPDE3A and mutant S^{654}A-PDE3A. *B*, however, only wtPDE3A is phosphorylated at S^{654} when cells were treated with 8-bromo-cGMP (4 h). *C*, the activity of wtPDE3A was also downregulated by PKG-Iα overexpression, whereas the S654A-mutant PDE3A was unaffected. *D*, similarly, cAMP levels were increased by PKG-Iα overexpression in cells expressing wtPDE3A but not in cells expressing the S^{654}A-PDE3A mutant. Data in *B* represent mean ± SEM, n = 3. *$p < 0.05$ wtPDE3A alone *versus* wtPDE3A + PKG-Iα; †$p < 0.05$ mutPDE3A + PKG-Iα *versus* wtPDE3A + PKG-Iα. Data in *C* and *D* represent mean ± SEM, n = 4. *$p < 0.05$ wtPDE3A alone *versus* wtPDE3A + PKG-Iα; †$p < 0.05$ wtPDE3A + PKG-Iα *versus* mutPDE3A + PKG-Iα. HEK293T, human embryonic kidney 293T cells; PDE3A, phosphodiesterase 3A; PKG-Iα, protein kinase G-Iα; S^{654}, serine 654.

regulatory protein vasodilator-stimulated phosphoprotein (VASP) at serine 239 (S^{239}) (34, 35). However, recent publications have identified VASP-S^{239}–independent effects of PKG-Iα in smooth muscle cells, suggesting other PKG-Iα–dependent regulatory mechanisms exist. These mechanisms may involve PKG-dependent phosphorylation of MYPT1, myosin light chain–targeting subunit of PP1 (36) and an inhibitory phosphorylation of RhoA (37). In this study, we show the involvement of PKG-Iα in the regulation of cAMP–cGMP signaling crosstalk *via* an inhibitory phosphorylation of the cAMP-degrading enzyme, PDE3A. The identified phosphorylation site, S^{654}, is present in the C-terminal region of PDE3A. Furthermore, we have confirmed that S^{654} phosphorylation status is crucial for PDE3A activity and intracellular levels of cAMP. Mutation of S^{654} to A^{654} produced a PDE3A mutant insensitive to PKG-Iα regulation. Recently, PKA and PKC phosphorylation events have been identified in PDE3A that stimulate its activity (38–40). The respective phosphorylation sites, serine 312 (S^{312}) and serine 428 (S^{428}), are present in the common N-terminal sequences in the PDE3A1 and PDE3A2 splice variants, whereas the shorter PDE3A3 variant lacks the N-terminal region containing S^{312} and S^{428} and cannot be modulated by PKA and PKC (40). Interestingly, PDE3A1 is mainly phosphorylated by PKA at S^{312}, whereas PDE3A2 is mainly phosphorylated by PKC at S^{428}. This difference in regulation determines further specificity in protein–protein interactions and PDE3A stability (40). In contrast, S^{654} is located in the common C-terminal region of PDE3A, and, therefore, all three variants of the PDE3A enzyme could be inhibited by PKG-Iα phosphorylation. However, further studies will be required to investigate this possibility.

Inhibition of cyclic nucleotide–specific PDEs is a therapeutic approach for a number of pathological states (41, 42). Cyclic nucleotide–dependent cell signaling plays an important role in the endothelial barrier–protective role in both cellular and animal models of ALI–ARDS (13, 43). Various compounds activating adenylate cyclase and, respectively, stimulating cAMP synthesis (such as purine receptor agonists) are protective against effects of LPS or other barrier-compromising factors *in vitro* and *in vivo* (13, 43–45). However, this effect is rather transient, since cyclic nucleotides can be rapidly degraded by specific PDEs. Moreover, some cAMP effectors can actually stimulate PDE isoforms allowing the termination of the signaling cascade (46). Therefore, active cAMP-specific PDEs may be involved in the direct inhibition of cAMP production. In our study of crosstalk in cyclic nucleotides in ALI, we evaluated the activities of the three families of PDEs that regulate cAMP–cGMP crosstalk in the vasculature: PDE2, PDE3A, and PDE5 (26, 28). It is well documented that PDEs 2, 3, and 5 are involved in the modulation of cGMP-dependent cell signaling. PDE2 is cGMP-specific PDE, whereas PDE5 is cGMP-activated cAMP-specific PDE (28). Our data show a specific perturbance of cyclic nucleotide signaling in LPS-exposed lung tissues. We found that LPS exposure activated PDE3A and inhibited PDE5. As a result, cAMP levels are diminished, and cGMP levels are elevated. However, cGMP elevation did not result in PKG-Iα activation because of the inhibitory effect of a peroxynitrite-induced modification resulting in the nitration of the protein at Y^{247} nitration.

PDE3 is one of the critical regulators of cAMP-dependent signaling cascades. It is rather unique among other cAMP-specific PDEs because of its very low K_m toward cAMP as a substrate (47), which indicates that PDE3 is able to regulate basal levels of cAMP, and its activation does not depend on an increase in intracellular cAMP concentration. In contrast, other cAMP-specific PDEs require high levels of cAMP for an efficient downregulation of cAMP signaling. Together, this suggests that PDE3 may be particularly critical for the efficient downregulation of stimuli-induced cAMP signaling as it will already be active at early stages of the cAMP induction process. In addition, recent studies have revealed PDE3 specificity toward cUMP, novel cyclic nucleotide secondary messenger involved in the regulation of PKG–PKA activities (reviewed in Ref. (48)). However, the importance of cUMP in the regulation of the endothelial function and pulmonary pathology will require further investigation. Recently, intracellular compartmentalization of PDE3A has been shown to exist, and its involvement in signalosome complexes suggests it plays an important role in fine tuning of cyclic nucleotide–induced signaling (49). PDE3 activity is also critical for the regulation of endothelial permeability *via* cytoskeletal rearrangements. Thus, the inhibition of PDE3 itself may have the barrier-enhancing effects. Indeed, in primary rat brain capillary endothelial cells and human brain microvascular endothelial cells, treatment with the PDE3 inhibitor, cilostazol, led to reorganization of F-actin, a dramatic increase in the expression of the tight junction protein, claudin-5, and barrier enhancement (50, 51). Cilostazol treatment also protected the barrier integrity of human brain microvascular endothelial cells from ethanol-induced disruption (52). The effects of cilostazol are abolished by PKA inhibition (50–52), suggesting that PDE3 inhibition increases basal levels of cAMP and stimulates PKA-dependent signaling. Therefore, PKG-Iα–dependent control of PDE3A activity *via* S^{654} phosphorylation in pulmonary endothelium could be absolutely critical for maintaining barrier integrity. Conversely, LPS-induced inhibition of PKG-Iα *via* Y^{247} nitration may be sufficient to initiate endothelial barrier disruption secondary to PDE3A activation and a decrease in cAMP levels.

PKG-Iα has been shown to act as redox effector, since under oxidative stress conditions, the enzyme is activated by dimerization *via* S–S bond formation (53, 54). This activation occurs in the absence of cGMP (53, 54) and is considered to be a cell-defensive mechanism. However, in ALI, when oxidative stress is also accompanied by increases in peroxynitrite formation, nitration of Y^{247} ultimately leads to PKG-Iα inhibition, and we show here that Y^{247} nitration, which impairs binding of cGMP by PKG-Iα (17), keeps the protein kinase in an inactive state even in the presence of cGMP. This inhibition likely plays a role in the endothelial barrier dysfunction associated with LPS, at least in part, through the resulting increase in PDE3A activity and the subsequent increased degradation of cAMP.

Basal cAMP levels are important in maintaining the endothelial barrier, and ALI-induced endothelial integrity loss is characterized by decreases in intracellular cAMP (14, 15) followed by inhibition of the barrier-protective effectors PKA and Epac-1 as well as small GTPase, Rac-1, all of which have been shown to be critical for maintaining endothelial integrity (55). Furthermore, our data suggest that under normal physiological conditions, PKG-Iα controls basal levels of cAMP. The protective effects of peroxynitrite scavenging in our experiments suggest a link between decreased PKG-Iα tyrosine nitration and the recovery of basal levels of cAMP.

Thus, in conclusion, we have elucidated a novel aspect of intracellular cAMP regulation *via* a cGMP-dependent pathway. This cyclic nucleotide crosstalk is regulated by cGMP-dependent PKG-Iα *via* an inhibitory phosphorylation of cAMP-specific PDE3A. Inhibition of PKG-Iα activity by nitration during ALI results in a dramatic loss of intracellular cAMP secondary to PDE3A activation, which is then followed by endothelial barrier disruption (summarized in Fig. 7). Finally, we speculate that the novel functional link described here may result in new approaches to ALI focused on preventing PKG-Iα nitration, thereby maintaining cAMP levels and leading to the protection of the pulmonary endothelial barrier.

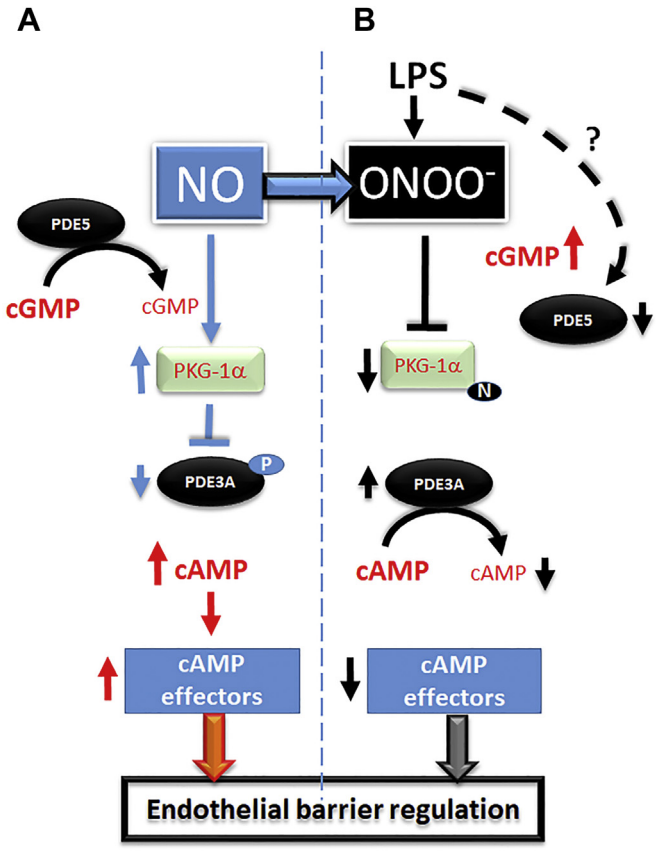

Figure 7. Schematic representation of PKG-Iα–dependent cAMP/cGMP crosstalk in pulmonary endothelial cells. *A*, under normal physiological conditions, NO-mediated cGMP generation activates PKG-Iα leading to inhibitory phosphorylation of PDE3A at S^{654}. This results in cAMP elevation and stimulation of barrier-enhancing effectors. *B*, LPS-mediated generation of peroxynitrite inhibits PKG-Iα *via* protein tyrosine nitration. Although cGMP levels are high because of LPS-dependent inhibition of PDE5, nitrated PKG-Iα cannot phosphorylate and inhibit PDE3A. This leads to PDE3A-dependent cAMP degradation and impaired barrier function. LPS, lipopolysaccharide; PDE3A, phosphodiesterase 3A; PKG-Iα, protein kinase G-Iα; NO, nitric oxide; S^{654}, serine 654.

Experimental procedures

Materials

Goat polyclonal anti-PKG-Iα antibodies were from Santa Cruz Biotechnology; mouse monoclonal antinitrotyrosine antibody (clone: CC22.8C7.3) was from EMD Biosciences, Inc; rabbit polyclonal anti-pSer^{239}VASP, rabbit polyclonal anti-VASP, rabbit polyclonal anti-PKAcat, and rabbit polyclonal PDE5 antibodies were from Cell Signaling; rabbit polyclonal anti-PDE2A antibodies were from Abcam; rabbit polyclonal anti-PDE3A antibodies were from LS Bio; mouse monoclonal anti-ß-actin antibody (clone: AC-15) and MnTMPyP were from Sigma Life Sciences; cGMP/AMP EIA Kits, 8-bromo-cGMP, and DHR were from Cayman Chemical; and a nonradioisotopic kit for measuring PKG activity was from Cyclex Co, Ltd. The Y^{247}-nitration–specific PKG-Iα antibody was generated as described (17). Phospho-S^{654}–specific PDE3A antibody was generated in rabbits by GenScript using a peptide derived from human PDE3A protein sequence (NP_000912), PLRKA(pS^{654})ACSTYAPE, as an antigen.

Measurement of peroxynitrite levels

The formation of peroxynitrite ($ONOO^-$) was determined by the $ONOO^-$-dependent oxidation of DHR123 to rhodamine 123 in peripheral lung tissue obtained from control and LPS-exposed mice (56). Tissues were pulverized; 10 mg of tissue was placed in a microfuge tube, 100 µl of PBS was added, and vortexed three times for 10 s. The lysate was incubated with PEG-labeled catalase (100 U) to reduce hydrogen peroxide–dependent DHR123 oxidation, for 30 min and then added to a 96-well black plate in the presence of 5 µmol/l DHR123 in PBS for 1 h. In both cases, the fluorescence of rhodamine 123 was measured at excitation 485 nm and emission 545 nm using a Fluoroskan Ascent Microplate Fluorometer (ThermoFisher Scientific).

Immunoblotting analysis

Cells or peripheral lung tissue were lysed in Triton X-100 lysis buffer (containing protease and phosphatase inhibitors), centrifuged at 6000*g*, and the supernatant was collected as previously described (57, 58). Tissue and cell extracts (25 µg) were resolved using 4 to 20% SDS-PAGE, electrophoretically transferred to Immuno-Blot PVDF membrane (Bio-Rad Laboratories), and blocked with 5% nonfat dry milk in Tris-buffered saline with 0.1% Tween-20. The membranes were probed with respective primary and secondary antibodies. Reactive protein bands were visualized using chemiluminescence (Pierce Laboratories) using either a Kodak 440CF image station or LI-COR Odyssey image station. Bands were quantified using either Kodak 1D image processing

software or LI-COR Image Station software. Expression was normalized by reprobing membranes with anti β-actin.

IP analysis

Cells or lung tissues were homogenized in 3× weight/volume of IP buffer (25 mM Hepes, pH 7.5, 150 mM NaCl, 1% NP-40, 10 mM $MgCl_2$, 1 mM EDTA, 2% glycerol, and supplemented with protease and phosphatase inhibitors). Homogenates were centrifuged at 20,000*g* at 4 °C for 10 min, the supernatants were collected, and protein concentrations were quantified using Bio-Rad DC Protein Assay (Bio-Rad Laboratories). To 1000 μg of total protein, 4 μg of antibodies were added; the volumes were adjusted to 1 ml with IP buffer, and the mixtures were rotated at 4 °C overnight. To precipitate the protein–antibody complexes, 30 μl of protein G plus agarose suspension (EMD Biosciences, Inc) were added, and the samples were rotated for 2 h at 4 °C. To collect the bead-bound complexes, the samples were centrifuged at 2000*g* for 5 min, the supernatants were discarded, and the beads were washed three times with 0.5 ml of IP buffer. Then 30 μl of 2× Laemmli buffer were added to each sample, and the samples were boiled for 5 min and analyzed by 4 to 20% Tris–SDS–Hepes PAGE followed by immunoblotting.

Determination of PKG and PKA activities

Total PKG activity was determined using a nonradioactive immunoassay to measure PKG-mediated phosphorylation of a synthetic substrate, according to the manufacturer's directions and as described (17). 8-Br cGMP was used to activate PKG to ensure that endogenous cGMP was not a limiting factor, as per the manufacturer's instructions. The results were expressed as picomoles of phosphate incorporated into the glutathione-*S*-transferase-G substrate fusion protein in the presence of cGMP (10 μM) per minute per microgram of total protein (pmol/min/μg) at 30 °C. PKA activity was evaluated in tissue extracts using PepTag Non-Radioactive PKA assay (Promega) according to the manufacturer's manual.

Measurement of cAMP and cGMP levels

Cells were lysed in 0.1 M HCl, and the supernatant was collected by centrifugation at 1000*g* for 10 min. Subsequently, cGMP–cAMP levels were measured using immunoassay-based EIA kits (Cayman Chemical), according to the manufacturer's protocol.

For tissue cGMP–cAMP determinations, lung tissue samples were snap frozen in liquid nitrogen and stored at −80 °C until use. For the assays, the tissues were ground into a fine powder under liquid nitrogen. Powdered samples were weighed, homogenized, and dissolved in 10 volumes of 0.1 M HCl, yielding units of picograms/milliliter, and centrifuged at 6000*g* at RT. cGMP levels were measured with the Assay Design EIA direct cGMP kit, acetylated version (Assay Design), according to the manufacturer's instructions.

Cell culture

HEK293T cells were grown in Dulbecco's modified Eagle's medium supplemented with 10% fetal bovine serum, 1% antibiotics–antimycotics at 37 °C in a humidified atmosphere with 5% CO_2. For transient transfection, Effectene (Qiagen) or ViaFect (Promega) transfection reagents were used according to the manufacturer's instructions. To stimulate protein tyrosine nitration, the cells were treated with 500 μM 3-morpholinosydnonimine (peroxynitrite generator) for 1 h.

PDE activity assays

Determination of PDE5 activity

For determination of PDE5 activity, mouse peripheral lung extracts (~25 μg) were incubated in the presence of dimethyl sulfoxide (DMSO) or the PDE5 inhibitor, sildenafil (1 μM), for 1 h at RT in a 1.5-ml microfuge tube. The levels of cGMP were measured using an immunoassay-based EIA kit, according to the manufacturer's protocol. The difference between cGMP levels in samples in the presence and absence of sildenafil was presumed to be the cGMP degraded by PDE5 and therefore a readout of PDE5 activity. The results were reported as femtomoles of cGMP degraded per minute at 25 °C per microgram of total protein (fmol/min/μg).

Determination of PDE2 and PDE3 activity

PDE3 and PDE2 activity was determined in mouse peripheral lung extracts, and PDE3 activity was determined in HEK293T cell lysates using the Bridge-It cAMP PDE Assay kit. For determination of PDE3 activity, equal protein (~25 μg) from each sample was incubated in the presence of DMSO or the PDE3 inhibitor, cilostamide (50 μM), for 1 h at RT in a 1.5-ml microfuge tube. Similarly, for determination of PDE2 activity, equal protein (~25 μg) from each sample was incubated in the presence of DMSO or the PDE2 inhibitor, BAY-60 to 7550 (2 μM), for 1 h at RT in a 1.5-ml microfuge tube. Subsequently, cAMP (600 nM) and PDE reaction buffer were added, and the mixture was incubated for 1 h at RT. The reaction was stopped, PDE assay solution was added, and the mixture was transferred to a 96-well black plate. After 30 min, the fluorescence intensity was read at excitation/emission 490/535 nm in a Fluoroskan Ascent Microplate Fluorometer. The concentrations of cAMP in each duplicate sample were determined through extrapolation from a standard curve, according to the manufacturer's instructions. The difference between cAMP levels in samples in the presence and absence of the specific PDE inhibitor was presumed to be the cAMP degraded by the respective PDE and therefore a readout of either PDE3 or PDE2 activity. The results were reported as femtomoles of cAMP degraded per minute at 25 °C per microgram of total protein (fmol/min/μg).

Animals

All animal housing protocols were approved by the Institutional Animal Care and Use Committee in facilities accredited by American Association for the Accreditation of

Laboratory Animal Care at Augusta University and the University of Arizona. Mice were injected intraperitoneally with *Escherichia coli* 0111:B4 lipopolysaccharide (6.75×10^4 EU/g body weight; Sigma–Aldrich) prepared in 0.9% saline, whereas control mice received vehicle (0.9% saline). Mice were euthanized 12 h after lipopolysaccharide injection, and the lungs were flushed with ice-cold EDTA–PBS, excised, snap frozen in liquid nitrogen, and stored at −80 °C until used.

MALDI-TOF MS

PDE3A and PKG-Iα constructs were transiently transfected in HEK293 cells for 48 h. PDE3A was immunoprecipitated from the cell lysates as described previously. The protein was resolved using 4 to 20% Tris–glycine SDS-PAGE and visualized by colloidal Coomassie stain (Bio-Rad Laboratories). The band corresponding to PDE3A (approximately 130 kDa) was excised and destained with 100 mM ammonium bicarbonate/50% (v/v) acetonitrile. Protein in gel was subjected to reduction and alkylation of cysteine residues before overnight in-gel digestion with chymotrypsin in 100 mM Tris–HCl containing 10 mM $CaCl_2$. The peptides were extracted with 0.1% TFA, 60% acetonitrile, and evaporated to near dryness. MS analysis of PDE3A was then performed as described (59). All spectra were taken on an ABSciex 5800 MALDI-TOF mass spectrometer in positive reflector mode (10 kV) with a matrix of cyano-4-hydroxycinnamic acid. At least 1000 laser shots were averaged to get each spectrum. The masses were calibrated to known peptide standards. The MS spectra were analyzed in the ProteinPilot software package (AB Sciex).

Statistical analysis

Statistical calculations were performed using the GraphPad Prism software (GraphPad Software, Inc). The mean ± SEM was calculated for all samples. Statistical significance was determined either by the unpaired *t* test (for two groups) or ANOVA (for three and/or more groups) with Newman–Keuls post hoc testing. A value of $p < 0.05$ was considered significant.

Data availability

All data for this publication are included in the article.

Author contributions—S. M. B. conceptualization; E. A. Z., X. W., S. A., M. Y., C. G., and H. W. methodology; E. A. Z., X. W., S. A., M. Y., C. G., H. W., and H. T. formal analysis; E. A. Z., X. W., S. A., M. Y., C. G., and H. W. investigation; X. W., M. Y., Q. L., H. W., and S. M. B. data curation; E. A. Z. writing-original draft; E. A. Z., X. W., S. A., M. Y., C. G., Q. L., H. W., H. T., and T. W. writing-review and editing; E. A. Z. and S. M. B. project administration; E. A. Z. and S. M. B. funding acquisition.

Funding and additional information—This research was supported in part by HL60190 (S. M. B.), HL137282 (S. M. B.), HL134610 (S. M. B.), HL142212 (S. M. B./E. A. Z.), HL146369 (S. M. B.), and the Interdisciplinary Training in Cardiovascular Research T32 HL007249 (X. W.), all from the National Heart, Lung, and Blood Institute, Bethesda, MD, USA.

Conflict of interest—The authors declare that they have no conflicts of interest with the contents of this article.

Abbreviations—The abbreviations used are: ALI, acute lung injury; ARDS, acute respiratory distress syndrome; DHR123, dihydrorhodamine 123; DMSO, dimethyl sulfoxide; HEK293T, human embryonic kidney 293T; LPS, lipopolysaccharide; MnTMPyP, manganese (III) tetrakis(1-methyl-4-pyridyl)porphyrin; PDE2, phosphodiesterase 2; PDE3, phosphodiesterase 3; PDE5, phosphodiesterase 5; PKG-Iα, protein kinase G-Iα; S^{239}, serine 239; S^{312}, serine 312; S^{428}, serine 428; S^{654}, serine 654; VASP, vasodilator-stimulated phosphoprotein; Y^{247}, tyrosine 247.

References

1. Beavo, J. A., and Brunton, L. L. (2002) Cyclic nucleotide research – still expanding after half a century. *Nat. Rev. Mol. Cell Biol.* **3**, 710–718
2. Davel, A. P., Victorio, J. A., Delbin, M. A., Fukuda, L. E., and Rossoni, L. V. (2015) Enhanced endothelium-dependent relaxation of rat pulmonary artery following beta-adrenergic overstimulation: Involvement of the NO/cGMP/VASP pathway. *Life Sci.* **125**, 49–56
3. Lincoln, T. M., Wu, X., Sellak, H., Dey, N., and Choi, C. S. (2006) Regulation of vascular smooth muscle cell phenotype by cyclic GMP and cyclic GMP-dependent protein kinase. *Front. Biosci.* **11**, 356–367
4. Nakane, M. (2003) Soluble guanylyl cyclase: Physiological role as an NO receptor and the potential molecular target for therapeutic application. *Clin. Chem. Lab. Med.* **41**, 865–870
5. Silver, P. J. (1985) Regulation of contractile activity in vascular smooth muscle by protein kinases. *Rev. Clin. Basic Pharm.* **5**, 341–395
6. Vogel, S. M., and Malik, A. B. (2012) Cytoskeletal dynamics and lung fluid balance. *Compr. Physiol.* **2**, 449–478
7. Garcia-Morales, V., Cuinas, A., Elies, J., and Campos-Toimil, M. (2014) PKA and Epac activation mediates cAMP-induced vasorelaxation by increasing endothelial NO production. *Vascul. Pharmacol.* **60**, 95–101
8. Goeckeler, Z. M., and Wysolmerski, R. B. (2005) Myosin phosphatase and cofilin mediate cAMP/cAMP-dependent protein kinase-induced decline in endothelial cell isometric tension and myosin II regulatory light chain phosphorylation. *J. Biol. Chem.* **280**, 33083–33095
9. Kellner, M., Noonepalle, S., Lu, Q., Srivastava, A., Zemskov, E., and Black, S. M. (2017) ROS signaling in the pathogenesis of acute lung injury (ALI) and acute respiratory distress syndrome (ARDS). *Adv. Exp. Med. Biol.* **967**, 105–137
10. Liu, H., Yu, X., Yu, S., and Kou, J. (2015) Molecular mechanisms in lipopolysaccharide-induced pulmonary endothelial barrier dysfunction. *Int. Immunopharmacol.* **29**, 937–946
11. Aslam, M., Hartel, F. V., Arshad, M., Gunduz, D., Abdallah, Y., Sauer, H., Piper, H. M., and Noll, T. (2010) cAMP/PKA antagonizes thrombin-induced inactivation of endothelial myosin light chain phosphatase: Role of CPI-17. *Cardiovasc. Res.* **87**, 375–384
12. Birukova, A. A., Xing, J., Fu, P., Yakubov, B., Dubrovskyi, O., Fortune, J. A., Klibanov, A. M., and Birukov, K. G. (2010) Atrial natriuretic peptide attenuates LPS-induced lung vascular leak: Role of PAK1. *Am. J. Physiol. Lung Cell Mol. Physiol.* **299**, L652–L663
13. Gonzales, J. N., Gorshkov, B., Varn, M. N., Zemskova, M. A., Zemskov, E. A., Sridhar, S., Lucas, R., and Verin, A. D. (2014) Protective effect of adenosine receptors against lipopolysaccharide-induced acute lung injury. *Am. J. Physiol. Lung Cell Mol. Physiol.* **306**, L497–L507
14. Schlegel, N., Baumer, Y., Drenckhahn, D., and Waschke, J. (2009) Lipopolysaccharide-induced endothelial barrier breakdown is cyclic adenosine monophosphate dependent *in vivo* and *in vitro*. *Crit. Care Med.* **37**, 1735–1743

15. Schlegel, N., and Waschke, J. (2009) Impaired cAMP and Rac 1 signaling contribute to TNF-alpha-induced endothelial barrier breakdown in microvascular endothelium. *Microcirculation* **16**, 521–533
16. Rafikov, R., Dimitropoulou, C., Aggarwal, S., Kangath, A., Gross, C., Pardo, D., Sharma, S., Jezierska-Drutel, A., Patel, V., Snead, C., Lucas, R., Verin, A., Fulton, D., Catravas, J. D., and Black, S. M. (2014) Lipopolysaccharide-induced lung injury involves the nitration-mediated activation of RhoA. *J. Biol. Chem.* **289**, 4710–4722
17. Aggarwal, S., Gross, C. M., Rafikov, R., Kumar, S., Fineman, J. R., Ludewig, B., Jonigk, D., and Black, S. M. (2014) Nitration of tyrosine 247 inhibits protein kinase G-1alpha activity by attenuating cyclic guanosine monophosphate binding. *J. Biol. Chem.* **289**, 7948–7961
18. Kumar, S., Sun, X., Noonepalle, S. K., Lu, Q., Zemskov, E., Wang, T., Aggarwal, S., Gross, C., Sharma, S., Desai, A. A., Hou, Y., Dasarathy, S., Qu, N., Reddy, V., Lee, S. G., *et al.* (2017) Hyper-activation of pp60(Src) limits nitric oxide signaling by increasing asymmetric dimethylarginine levels during acute lung injury. *Free Radic. Biol. Med.* **102**, 217–228
19. Sharma, S., Smith, A., Kumar, S., Aggarwal, S., Rehmani, I., Snead, C., Harmon, C., Fineman, J., Fulton, D., Catravas, J. D., and Black, S. M. (2010) Mechanisms of nitric oxide synthase uncoupling in endotoxin-induced acute lung injury: Role of asymmetric dimethylarginine. *Vascul. Pharmacol.* **52**, 182–190
20. Baillie, G. S. (2009) Compartmentalized signalling: Spatial regulation of cAMP by the action of compartmentalized phosphodiesterases. *FEBS J.* **276**, 1790–1799
21. Houslay, M. D., and Milligan, G. (1997) Tailoring cAMP-signalling responses through isoform multiplicity. *Trends Biochem. Sci.* **22**, 217–224
22. Stangherlin, A., and Zaccolo, M. (2012) Phosphodiesterases and subcellular compartmentalized cAMP signaling in the cardiovascular system. *Am. J. Physiol. Heart Circ. Physiol.* **302**, H379–H390
23. Lynch, M. J., Baillie, G. S., and Houslay, M. D. (2007) cAMP-specific phosphodiesterase-4D5 (PDE4D5) provides a paradigm for understanding the unique non-redundant roles that PDE4 isoforms play in shaping compartmentalized cAMP cell signalling. *Biochem. Soc. Trans.* **35**, 938–941
24. Masciarelli, S., Horner, K., Liu, C., Park, S. H., Hinckley, M., Hockman, S., Nedachi, T., Jin, C., Conti, M., and Manganiello, V. (2004) Cyclic nucleotide phosphodiesterase 3A-deficient mice as a model of female infertility. *J. Clin. Invest.* **114**, 196–205
25. Zuo, H., Han, B., Poppinga, W. J., Ringnalda, L., Kistemaker, L. E. M., Halayko, A. J., Gosens, R., Nikolaev, V. O., and Schmidt, M. (2018) Cigarette smoke up-regulates PDE3 and PDE4 to decrease cAMP in airway cells. *Br. J. Pharmacol.* **175**, 2988–3006
26. Pavlaki, N., and Nikolaev, V. O. (2018) Imaging of PDE2- and PDE3-mediated cGMP-to-cAMP cross-talk in cardiomyocytes. *J. Cardiovasc. Dev. Dis.* **5**, 4
27. Zaccolo, M., and Movsesian, M. A. (2007) cAMP and cGMP signaling cross-talk: Role of phosphodiesterases and implications for cardiac pathophysiology. *Circ. Res.* **100**, 1569–1578
28. Maurice, D. H. (2005) Cyclic nucleotide phosphodiesterase-mediated integration of cGMP and cAMP signaling in cells of the cardiovascular system. *Front. Biosci.* **10**, 1221–1228
29. Pooladanda, V., Thatikonda, S., Bale, S., Pattnaik, B., Sigalapalli, D. K., Bathini, N. B., Singh, S. B., and Godugu, C. (2019) Nimbolide protects against endotoxin-induced acute respiratory distress syndrome by inhibiting TNF-alpha mediated NF-kappaB and HDAC-3 nuclear translocation. *Cell Death Dis.* **10**, 81
30. Ricciardolo, F. L., Sorbello, V., Benedetto, S., and Paleari, D. (2015) Effect of ambroxol and beclomethasone on lipopolysaccharide-induced nitrosative stress in bronchial epithelial cells. *Respiration* **89**, 572–582
31. Hwang, T. L., Tang, M. C., Kuo, L. M., Chang, W. D., Chung, P. J., Chang, Y. W., and Fang, Y. C. (2012) YC-1 potentiates cAMP-induced CREB activation and nitric oxide production in alveolar macrophages. *Toxicol. Appl. Pharmacol.* **260**, 193–200
32. Joshi, C. N., Martin, D. N., Fox, J. C., Mendelev, N. N., Brown, T. A., and Tulis, D. A. (2011) The soluble guanylate cyclase stimulator BAY 41-2272 inhibits vascular smooth muscle growth through the cAMP-dependent protein kinase and cGMP-dependent protein kinase pathways. *J. Pharmacol. Exp. Ther.* **339**, 394–402
33. Ramos-Espiritu, L. S., Hess, K. C., Buck, J., and Levin, L. R. (2011) The soluble guanylyl cyclase activator YC-1 increases intracellular cGMP and cAMP via independent mechanisms in INS-1E cells. *J. Pharmacol. Exp. Ther.* **338**, 925–931
34. Adderley, S. P., Joshi, C. N., Martin, D. N., and Tulis, D. A. (2012) Phosphodiesterases regulate BAY 41-2272-induced VASP phosphorylation in vascular smooth muscle cells. *Front. Pharmacol.* **3**, 10
35. Samuel, S., Zhang, K., Tang, Y. D., Gerdes, A. M., and Carrillo-Sepulveda, M. A. (2017) Triiodothyronine potentiates vasorelaxation via PKG/VASP signaling in vascular smooth muscle cells. *Cell Physiol. Biochem.* **41**, 1894–1904
36. Lubomirov, L. T., Papadopoulos, S., Filipova, D., Baransi, S., Todorovic, D., Lake, P., Metzler, D., Hilsdorf, S., Schubert, R., Schroeter, M. M., and Pfitzer, G. (2018) The involvement of phosphorylation of myosin phosphatase targeting subunit 1 (MYPT1) and MYPT1 isoform expression in NO/cGMP mediated differential vasoregulation of cerebral arteries compared to systemic arteries. *Acta Physiol. (Oxf.)* **224**, e13079
37. Zhao, Y. D., Cai, L., Mirza, M. K., Huang, X., Geenen, D. L., Hofmann, F., Yuan, J. X., and Zhao, Y. Y. (2012) Protein kinase G-I deficiency induces pulmonary hypertension through Rho A/Rho kinase activation. *Am. J. Pathol.* **180**, 2268–2275
38. Geoffroy, V., Fouque, F., Nivet, V., Clot, J. P., Lugnier, C., Desbuquois, B., and Benelli, C. (1999) Activation of a cGMP-stimulated cAMP phosphodiesterase by protein kinase C in a liver Golgi-endosomal fraction. *Eur. J. Biochem.* **259**, 892–900
39. Palmer, D., Jimmo, S. L., Raymond, D. R., Wilson, L. S., Carter, R. L., and Maurice, D. H. (2007) Protein kinase A phosphorylation of human phosphodiesterase 3B promotes 14-3-3 protein binding and inhibits phosphatase-catalyzed inactivation. *J. Biol. Chem.* **282**, 9411–9419
40. Vandeput, F., Szabo-Fresnais, N., Ahmad, F., Kho, C., Lee, A., Krall, J., Dunlop, A., Hazel, M. W., Wohlschlegel, J. A., Hajjar, R. J., Houslay, M. D., Manganiello, V. C., and Movsesian, M. A. (2013) Selective regulation of cyclic nucleotide phosphodiesterase PDE3A isoforms. *Proc. Natl. Acad. Sci. U. S. A.* **110**, 19778–19783
41. Fan Chung, K. (2006) Phosphodiesterase inhibitors in airways disease. *Eur. J. Pharmacol.* **533**, 110–117
42. Stehlik, J., and Movsesian, M. A. (2006) Inhibitors of cyclic nucleotide phosphodiesterase 3 and 5 as therapeutic agents in heart failure. *Expert Opin. Investig. Drugs* **15**, 733–742
43. Umapathy, N. S., Zemskov, E. A., Gonzales, J., Gorshkov, B. A., Sridhar, S., Chakraborty, T., Lucas, R., and Verin, A. D. (2010) Extracellular beta-nicotinamide adenine dinucleotide (beta-NAD) promotes the endothelial cell barrier integrity via PKA- and EPAC1/Rac1-dependent actin cytoskeleton rearrangement. *J. Cell Physiol.* **223**, 215–223
44. Umapathy, N. S., Fan, Z., Zemskov, E. A., Alieva, I. B., Black, S. M., and Verin, A. D. (2010) Molecular mechanisms involved in adenosine-induced endothelial cell barrier enhancement. *Vascul. Pharmacol.* **52**, 199–206
45. Zemskov, E., Lucas, R., Verin, A. D., and Umapathy, N. S. (2011) P2Y receptors as regulators of lung endothelial barrier integrity. *J. Cardiovasc. Dis. Res.* **2**, 14–22
46. Murthy, K. S., Zhou, H., and Makhlouf, G. M. (2002) PKA-dependent activation of PDE3A and PDE4 and inhibition of adenylyl cyclase V/VI in smooth muscle. *Am. J. Physiol. Cell Physiol.* **282**, C508–C517
47. Hambleton, R., Krall, J., Tikishvili, E., Honeggar, M., Ahmad, F., Manganiello, V. C., and Movsesian, M. A. (2005) Isoforms of cyclic nucleotide phosphodiesterase PDE3 and their contribution to cAMP hydrolytic activity in subcellular fractions of human myocardium. *J. Biol. Chem.* **280**, 39168–39174
48. Seifert, R. (2015) cCMP and cUMP: Emerging second messengers. *Trends Biochem. Sci.* **40**, 8–15
49. Guinzberg, R., Diaz-Cruz, A., Acosta-Trujillo, C., Vilchis-Landeros, M. M., Vazquez-Meza, H., Lozano-Flores, C., Chiquete-Felix, N., Varela-Echavarria, A., Uribe-Carvajal, S., Riveros-Rosas, H., and Pina, E. (2017) Newly synthesized cAMP is integrated at a membrane

protein complex signalosome to ensure receptor response specificity. *FEBS J.* **284**, 258–276
50. Horai, S., Nakagawa, S., Tanaka, K., Morofuji, Y., Couraud, P. O., Deli, M. A., Ozawa, M., and Niwa, M. (2013) Cilostazol strengthens barrier integrity in brain endothelial cells. *Cell Mol. Neurobiol.* **33**, 291–307
51. Liu, S., Yu, C., Yang, F., Paganini-Hill, A., and Fisher, M. J. (2012) Phosphodiesterase inhibitor modulation of brain microvascular endothelial cell barrier properties. *J. Neurol. Sci.* **320**, 45–51
52. Takagi, T., Mishiro, K., Shimazawa, M., Yoshimura, S., Iwama, T., and Hara, H. (2014) The phosphodiesterase III inhibitor cilostazol ameliorates ethanolinduced endothelial dysfunction. *Curr. Neurovasc. Res.* **11**, 302–311
53. Burgoyne, J. R., Madhani, M., Cuello, F., Charles, R. L., Brennan, J. P., Schroder, E., Browning, D. D., and Eaton, P. (2007) Cysteine redox sensor in PKGIa enables oxidant-induced activation. *Science* **317**, 1393–1397
54. Sheehe, J. L., Bonev, A. D., Schmoker, A. M., Ballif, B. A., Nelson, M. T., Moon, T. M., and Dostmann, W. R. (2018) Oxidation of cysteine 117 stimulates constitutive activation of the type Ialpha cGMP-dependent protein kinase. *J. Biol. Chem.* **293**, 16791–16802
55. Waschke, J., Drenckhahn, D., Adamson, R. H., Barth, H., and Curry, F. E. (2004) cAMP protects endothelial barrier functions by preventing Rac-1 inhibition. *Am. J. Physiol. Heart Circ. Physiol.* **287**, H2427–H2433
56. Song, P., Wu, Y., Xu, J., Xie, Z., Dong, Y., Zhang, M., and Zou, M. H. (2007) Reactive nitrogen species induced by hyperglycemia suppresses Akt signaling and triggers apoptosis by upregulating phosphatase PTEN (phosphatase and tensin homologue deleted on chromosome 10) in an LKB1-dependent manner. *Circulation* **116**, 1585–1595
57. Sharma, S., Sud, N., Wiseman, D. A., Carter, A. L., Kumar, S., Hou, Y., Rau, T., Wilham, J., Harmon, C., Oishi, P., Fineman, J. R., and Black, S. M. (2008) Altered carnitine homeostasis is associated with decreased mitochondrial function and altered nitric oxide signaling in lambs with pulmonary hypertension. *Am. J. Physiol. Lung Cell Mol. Physiol.* **294**, L46–L56
58. Sud, N., Sharma, S., Wiseman, D. A., Harmon, C., Kumar, S., Venema, R. C., Fineman, J. R., and Black, S. M. (2007) Nitric oxide and superoxide generation from endothelial NOS: Modulation by HSP90. *Am. J. Physiol. Lung Cell Mol. Physiol.* **293**, L1444–L1453
59. Aggarwal, S., Gross, C. M., Kumar, S., Datar, S., Oishi, P., Kalkan, G., Schreiber, C., Fratz, S., Fineman, J. R., and Black, S. M. (2011) Attenuated vasodilatation in lambs with endogenous and exogenous activation of cGMP signaling: Role of protein kinase G nitration. *J. Cell Physiol.* **226**, 3104–3113